Surface & Coatings Technology 205 (2010) S447–S450

Contents lists available at ScienceDirect

Surface & Coatings Technology

journal homepage: www.elsevier.com/locate/surfcoat

# Structural and optical properties of silicon by tilted angle evaporation

Sung Jun Jang [a], Young Min Song [a], Hee Ju Choi [b], Jae Su Yu [c], Yong Tak Lee [a,*]

[a] Department of Information and Communications, Gwangju Institute of Science and Technology, 1 Oryong-dong, Buk-gu, Gwanju 500-712, Republic of Korea
[b] School of Photon Science and Technology, Gwangju Institute of Science and Technology, 1 Oryong-dong, Buk-gu, Gwanju 500-712, Republic of Korea
[c] Department of Electronic and Radio Engineering, Kyung Hee University, 1 Seocheon-dong, Giheung-gu, Yongin 446-701, Republic of Korea

ARTICLE INFO

Available online 6 September 2010

*Keywords:*
Silicon
Tilted angle evaporation
Nanocolumn
RCWA
TMM

ABSTRACT

We fabricate the silicon (Si) films on Si substrate by using the tilted angle evaporation technique. The deposition rate of Si films is decreased with increasing the tilted angle of substrate. The refractive index (n) and extinction coefficient can be engineered by the introduction of the porosity into Si films. The refractive index of Si films is controllably varied from 3.4 to 1.6 in the visible wavelength range for different incident angles of Si flux. The extinction coefficient also becomes lower for the larger tilted angle. The porous Si films (i.e., low-n Si) with an inclined nanocolumn structure are observed after evaporation, depending on the incident angle of Si flux. The reflectance of deposited Si films on Si substrate is measured by a spectrophotometer in comparison with theoretical calculations by rigorous coupled-wave analysis and transfer matrix method. These reflectance results are well consistent with the simulated results obtained using the measured refractive index values of the deposited Si films.



## 1. Introduction

There is increasing interest in exploiting the capability of varying refractive index of films for applications including reflectors, antireflection coatings, filters, and resonators [1,2]. Compared to conventional multilayer stack films, graded refractive index homogeneous films can be less sensitive to the angle of incidence [3], and are thus desirable for use in optoelectronic devices such as solar cells and light-emitting diodes [4,5]. Various methods have been employed for the refractive index engineering of a single material: silicon oxynitrides ($SiO_xN_y$) grown by plasma-enhanced chemical vapor deposition [6], and $TiO_2$ and $SiO_2$ deposited by oblique angle deposition (OAD) [7]. The former can be fabricated easily by controlling the gas ratio of $O_2/N_2$, but the index variation range of $SiO_xN_y$ is too small to cover the whole refractive index range between the dielectric and air. The OAD is a dominant method for the fabrication of highly porous thin films. Thus, the letter can cover a relatively large refractive index range, but the thermal conductivities are very low for both $SiO_2$ and $TiO_2$ [8].

In the case of silicon (Si), the thermal conductivity is very high (i.e., 149 W/m K) [9], which is required for practical applications. The efficient heat dissipation is very essential for long-term wavelength stability and reliability of devices. The refractive index of Si can be controlled by the OAD method over a wide range due to the large difference in the refractive indices of air and Si substrate. Additionally, the OAD-based structure may change the surface reflection associated with the refractive index profile. The reflectance control allows for the optimal design of novel structures with efficient antireflection properties at specific wavelengths. In this paper, we report the structural and optical properties of Si fabricated by tilted angle evaporation. The effect of the tilted angle during deposition on the refractive index, extinction coefficient, and reflectance were investigated with the structural observation of porous Si films.

## 2. Experimental details

The Si films were deposited on (100) Si substrate by e-beam evaporator using a tilted angle evaporation method. Fig. 1 shows the

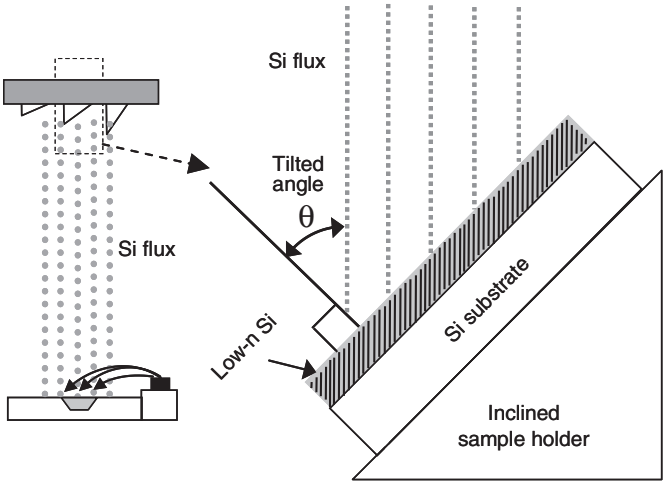


**Fig. 1.** Schematic illustration of experiment setup with inclined sample holders for the tilted angle evaporation of Si films.

* Corresponding author. Tel.: +82 62 970 2239.
*E-mail address:* ytlee@gist.ac.kr (Y.T. Lee).

0257-8972/$ – see front matter © 2010 Elsevier B.V. All rights reserved.
doi:10.1016/j.surfcoat.2010.08.131

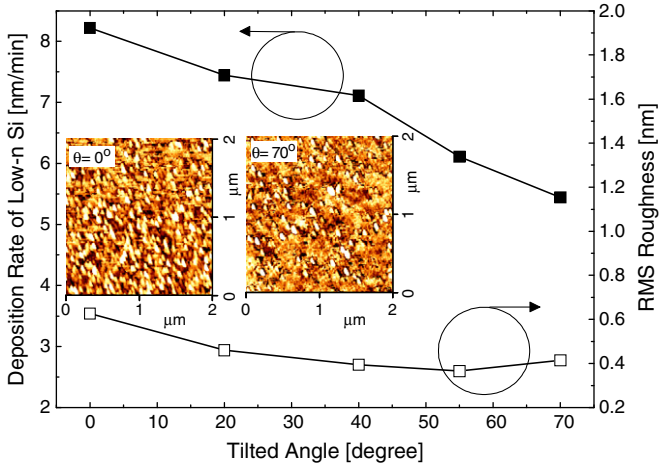


**Fig. 2.** Deposition rate and RMS roughness of low-n Si films as a function of tilted angle. The inset shows the 2 μm × 2 μm AFM scan images of the deposited Si films for θ = 0° and θ = 70°.

schematic illustration of experiment setup with inclined sample holders for the tilted angle evaporation of Si films. The Si pellets (99.999% purity) were melted in 7 $cm^3$ crucible and then evaporated with a 10 kV electron beam after a stable evaporation rate of Si. Since Si can be oxidized easily at pressures above $4 \times 10^{-6}$ Torr, the chamber was evacuated to a base pressure of $<1 \times 10^{-6}$ Torr by a cryogenic pump. The in situ deposition rate was roughly estimated using a quartz crystal sensor. For the tilted angle, the substrate was located on the inclined sample holders with 0°, 20°, 40°, 50°, 55°, and 70° angles to control the nanocolumn structure in the Si films. As shown in Fig. 1, the angle of inclined sample holder is matched with the incident angle (i.e., tilted angle θ) of the evaporated Si flux with respect to the Si substrate surface normal. The evaporation was performed without rotating the substrate. The target thickness of deposited Si films was kept at approximately 100 nm. The refractive index and extinction coefficient of Si were characterized by a spectroscopic ellipsometer. The structural and morphological properties of the deposited films were observed by a scanning electron microscope (SEM). The surface roughness was measured by an atomic force microscope (AFM). The reflectance spectra were measured by a UV–vis-IR spectrophotometer.

## 3. Results and discussion

Fig. 2 shows the deposition rate and root-mean-square (RMS) roughness of low-n Si films as a function of tilted angle. The inset shows the 2 μm × 2 μm AFM scan images of the deposited Si films for θ = 0° and θ = 70°. The thickness was measured by both SEM and spectroscopic ellipsometer and RMS roughness were measured by AFM. As the tilted angle was increased, the measured thickness of deposited Si films was decreased, thus reducing the deposition rate from 8.2 nm/min at θ = 0° to 5.4 nm/min at θ = 70°. This can be explained by the fact that the effectively reduced area of Si flux was mapped on the substrate with a larger tilted angle. Thus, there is a difference between the monitored film thickness by quartz crystal sensor and the actual thickness. The measured RMS roughness of film surface was varied over the range of ~0.4–0.6 nm for different tilted angles of θ = 0–70°.

Fig. 3 shows the cross-sectional SEM images of deposited Si films on Si substrate with tilted angles of (a) θ = 0°, (b) θ = 45°, (c) θ = 55°, and (d) θ = 70°. In tilted angle evaporation, the nonocolumn structure was observed and it was inclined away from the surface normal along the incident Si flux direction. By increasing the tilted angle, the column inclination was clearly increased and its structure became more distinct. Typically the evaporated Si flux flows perpendicularly from the source pocket to the Si substrate in the chamber of e-beam evaporator. Since the substrate has a specific angle with respect to the incident Si flux by an inclined sample holder, the evaporated Si sources can reach the substrate surface in a tilted state. The initial Si nucleation formed randomly leads to a self-alignment by preventing the incident flux from reaching the shadow region due to the self-shadowing effect [10], resulting in the inclined nanocolumn profile. It is clear that the thickness of deposited Si films is noticeably decreased at θ = 70°. The size of nanocolumns was ~10 nm–20 nm. The deposited Si film was somewhat dense in this experiment despite the tilted angle evaporation. This structural hardness may provide the

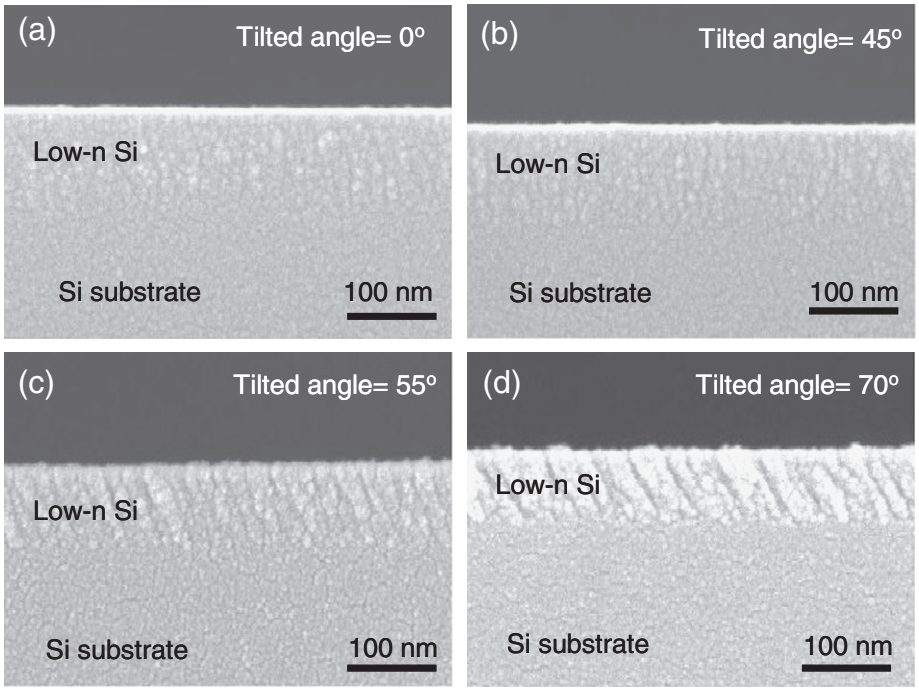


**Fig. 3.** Cross-sectional SEM images of deposited Si films on Si substrate with tilted angles of (a) θ = 0°, (b) θ = 45°, (c) θ = 55°, and (d) θ = 70°.

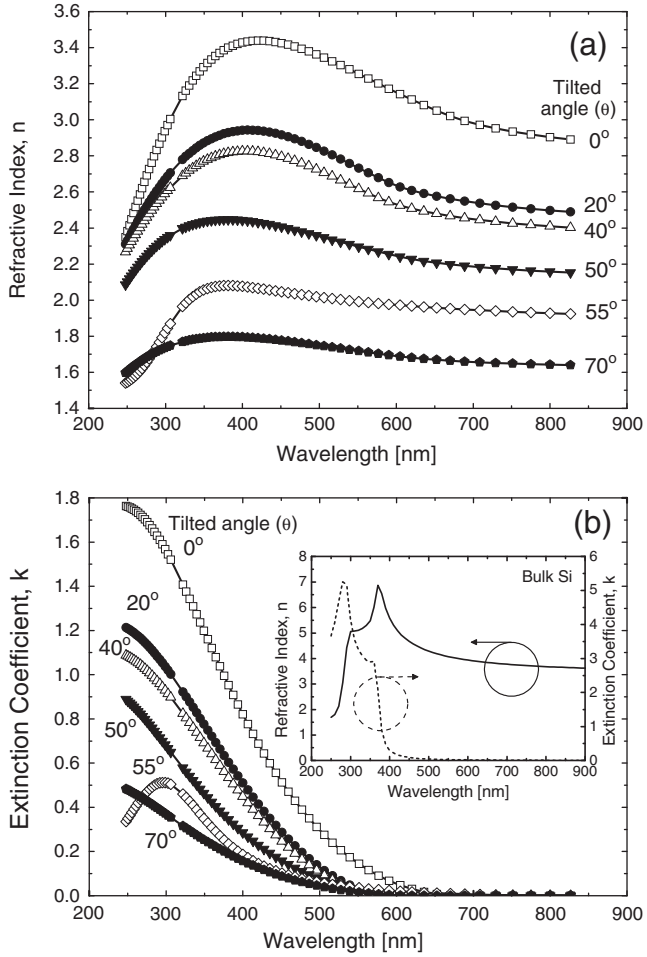


**Fig. 4.** (a) Refractive index and (b) extinction coefficient as a function of wavelength for deposited Si films with different tilted angles. The inset of (b) shows the refractive index and extinction coefficient spectra of a reference bulk Si [7].

mechanical stability for device applications. Nevertheless, the Si films seem to become more porous as the tilted angle is increased. It means that the amorphous Si with a low refractive index (n), i.e., non-crystalline Si, is formed by the tilted angle evaporation.

To investigate the effect of the porosity in deposited Si films, the ellipsometric measurements were performed. Fig. 4 shows (a) the refractive index and (b) the extinction coefficient as a function of wavelength for deposited Si films with different tilted angles. The refractive index and extinction coefficient spectra of a reference bulk Si [11] is also shown in the inset of Fig. 4(b). The refractive index was decreased from 3.4 to 1.6 in the visible wavelength range as the tilted angle was increased. Clearly, the reduction of refractive index is due to the increased porosity (i.e., air of $n=1$) within Si films from the inclined porous structure as shown in Fig. 3. The porous nature of inclined Si films produces a lower refractive index as a Bruggemann effective refractive medium [12] between the Si and the air, approaching to $n=1$ with a further increase in porosity. The maxima in refractive index spectra were shifted from 3.4 at 420 nm for $\theta=0°$ nm to 1.79 at 381 nm for $\theta=70°$ towards a shorter wavelength with increasing the tilted angle. At a wavelength of 635 nm, the refractive index was varied from 3.09 to 1.67 as the tilted angle was increased from $\theta=0°$ to $\theta=70°$. As shown in Fig. 4(b), the extinction coefficient was also decreased as the titled angle was increased. The extinction coefficient was very low in the wavelength region above 500 nm. For low-n Si films, the extinction coefficient is dramatically decreased, especially in the UV wavelength region. The value is almost similar to that of $SiN_x$ film [13]. It is event that the refractive index and extinction coefficient of the deposited Si films are significantly reduced by the tilted angle evaporation compared to the reference bulk Si as shown in the inset of Fig. 4(b).

Fig. 5 shows the measured and calculated reflectance as a function of wavelength for deposited Si films with tilted angles of (a) $\theta=0°$, (b) $\theta=45°$, (c) $\theta=55°$, and (d) $\theta=70°$. The reflectance spectra of bulk Si is also shown in Fig. 5(a). For theoretical analysis, the reflectance calculations of the low-n Si structures on Si substrate were carried out by the rigorous coupled-wave analysis (RCWA) and transfer matrix method (TMM) [14,15]. The measured refractive

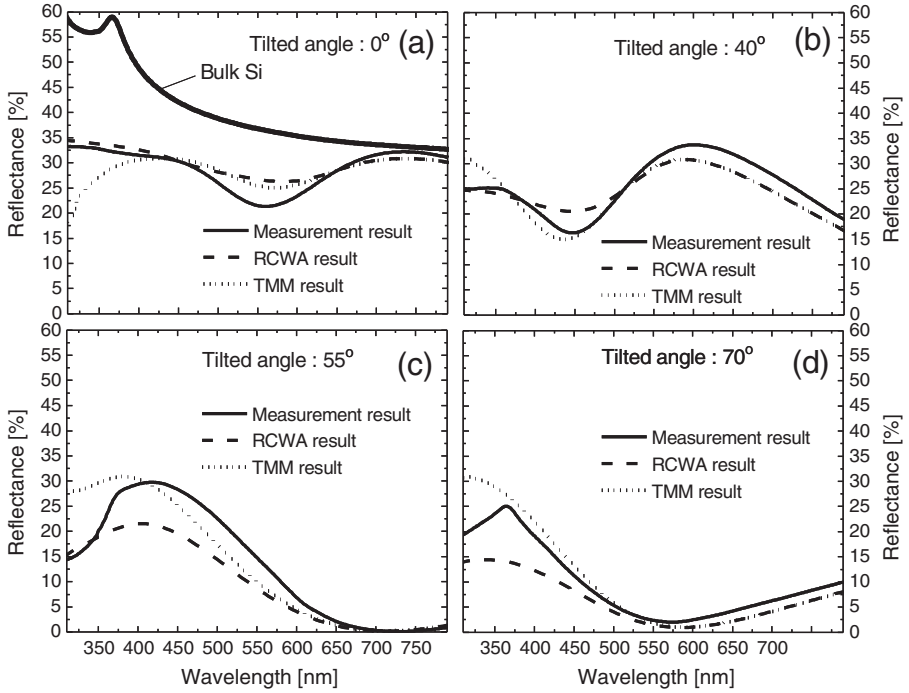


**Fig. 5.** Measured and calculated reflectance as a function of wavelength for deposited Si films with tilted angles of (a) $\theta=0°$, (b) $\theta=45°$, (c) $\theta=55°$, and (d) $\theta=70°$. The reflectance spectra of bulk Si is also shown in (a).

index values were used for low-n Si films. For bulk Si, the reflectance is very high with values above 32% in the visible wavelength range. The low-n Si films on an Si substrate exhibited the oscillation in reflectance spectra due to the multiple beam interference in the films. The slow oscillation is ascribed to the thin layer of ~100 nm. As shown in Fig. 5, the reflectance spectra were modified by the tilted angle evaporation. The reflectance was roughly reduced as the tilted angle was increased. For the tilted angle of $\theta = 55°$, the antireflective property was obtained at wavelengths above 600 nm. For the tilted angle of $\theta = 55°$, the reflectance of<10% was achieved over a wavelength range of 465–800 nm. The measured reflectance results agreed reasonably with the calculated results in the visible wavelength range though there is little discrepancy in the TMM results below 400 nm. This difference is caused by an error in refractive index of bulk Si in the UV wavelength region. From these results, the reflectance can be controlled by the tilted angle during evaporation over a wide wavelength range, together with careful theoretical calculations.

## 4. Conclusion

We studied the refractive index, extinction coefficient, and reflectance of low-n Si films on Si substrate by the tilted angle evaporation. It is found that the deposition rate was reduced with increasing the tilted angle. The optical properties depend strongly on the tilted angle. As the inclined angle was increased, the nanocolumn in deposited Si films was tilted away along the incident Si flux direction and the films became more porous from the SEM observation. The refractive index and extinction coefficient became lower with the increase of tilted angle due to the increased porosity within the Si films. The measured reflectance value of evaporated Si films was also dependant on the tilted angle and it was substantially reduced for the tilted angle of $\theta = 70°$ over a visible wavelength range, providing a good consistent with the results calculated theoretically using RCWA and TMM. These results will give a better understanding of the control mechanism of the structural and optical properties for the films deposited by the tilted angle evaporation.

## Acknowledgements

This work was supported by the Technology Innovation Program of the MKE, Korea [2007-F-045-03] and by the WCU program of MEST (Project No. R31-2008-000-10026-0). We thank K. Y. Oh for SEM measurements.

## References

[1] S. Larouche, L. Martinu, Appl. Opt. 47 (2008) 4321.
[2] H. Karimi-Alavijeh, G.M. Parsanasab, M.A. Baghban, E. Sarailou, A. Gharavi, Appl. Phys. Lett. 92 (2008) 041105.
[3] M.J. Minot, J. Opt. Soc. Am. 67 (1977) 1046.
[4] S. Chhajed, M.F. Schubert, J.K. Kim, E.F. Schubert, Appl. Phys. Lett. 93 (2008) 251108.
[5] W.H. Southwell, Opt. Lett. 8 (1983) 584.
[6] S. Callard, A. Gagnaire, J. Joseph, Thin Solid Films 313–314 (1998) 384.
[7] M. Kuo, et al., Opt. Lett. 33 (2008) 2527.
[8] D.G. Cahill, T.H. Allen, Appl. Phys. Lett. 65 (1994) 309.
[9] Y.S. Touloukian, R.W. Powell, C.Y. Ho, P.G. Klemens, Thermophys. Prop. Matter 1 (1970) 339.
[10] S.J. Jang, J.S. Yu, Y.T. Lee, IEEE Photon. Technol. Lett. 20 (2008) 514.
[11] M.A. Green, M. Keevers, Prog. Photovoltaics 3 (1995) 189.
[12] D.A.G. Bruggeman, Ann. Phys. 24 (1935) 636 (Leipzip).
[13] M. Lipinski, A. Kaminski, J.-F. Lelievre, M. Lemiti, E. Fourmond, P. Zieba, Phys. Phys. Status Solidi A 4 (2007) 1566.
[14] M.G. Moharam, T.K. Gaylord, J. Opt. Soc. Am. 71 (1981) 811.
[15] F.L. Pedrotti, L.M. Pedrotti, L.S. Pedrotti, Introduction to Optics, third edition, Pearson Prentice Hall, 2007, p. 476.